

SOURCES OF ENERGY FLEXIBILITY IN DISTRICT HEATING NETWORKS: BUILDING THERMAL INERTIA VERSUS THERMAL ENERGY STORAGE IN THE NETWORK PIPES

Annelies Vandermeulen^{1, 2, 3}, Glenn Reynders^{1, 2, 3}, Bram van der Heijde^{1, 2, 3}, Dirk Vanhoudt^{2, 3}, Robbe Salenbien^{2, 3}, Dirk Saelens^{1, 2} and Lieve Helsen^{1, 2}

¹University of Leuven, Leuven, Belgium

²EnergyVille, Genk, Belgium

³Vito, Mol, Belgium

ABSTRACT

An increasing share of intermittent renewable energy sources calls for more flexible energy systems. This flexibility - the capability of shifting energy use in time and/or magnitude - can be obtained, amongst others, by integration of thermal energy storage in district heating systems. Adequate control of storage systems allows increasing intermittent renewable energy supply and/or decreasing curtailment. In a district heating network, many different thermal energy storage systems are available, each with their own characteristics and dynamics. To facilitate an optimal selection and combination of these different storage systems, a flexibility characterization method was defined by IEA-EBC Annex 67. This paper verifies this characterization method by evaluating the energy flexibility provided by two sources inherently present in a district heating network, being the water thermal mass in the network pipes and the thermal inertia of the buildings connected to the network. The paper evaluates multiple scenarios, comparing different streets and small districts, and combining different dwelling types. The obtained energy flexibility characteristics shows that the network contribution is limited compared to that of the buildings' thermal inertia, at least in the case of small networks. Furthermore, results show that the non-linear characteristics of the district heating network, such as congestion, could complicate the aggregation of flexibility characteristics.

INTRODUCTION

The transition to a sustainable energy system with more renewable energy sources (RES) requires extensive changes to today's energy system. Especially the intermittency of RES makes the generation of electricity/heat hard to accurately predict or control and hence calls for a different approach. Energy flexibility at the demand side [1] introduces the capability to adapt the energy use at a given moment to reach a certain goal, such as the prevention of RES curtailment [2], peak shaving [3] or self-consumption of RES [4]. District heating and cooling networks, and thermal networks in general, can use energy flexibility to improve their own performance (e.g., peak shaving and valley filling [5], integration of RES [6], optimizing combined heat and power (CHP) and heat pump operation [7], etc.). On the other hand, thermal networks can also provide ancillary services to electricity networks by using the energy flexibility present in the thermal network [8].

Energy flexibility in thermal networks can be offered by thermal energy storage (TES), including dedicated storage systems, e.g. tanks and aquifers, and TES inherently present in the network, e.g. building thermal inertia [9] and the network pipes containing warm water [5]. In order to determine, compare and combine the available energy flexibility of the different TES systems, quantification methods are required. However, it appears that many different definitions and methods exist, varying from indicators quantifying different physical and technical aspects of energy flexibility [10], [11], over cost curves which link the energy flexibility to the cost of activation [12] to integrated evaluation of energy storage and optimal control [13]. An overview and comparison of these different techniques was made by Reynders *et al.* [14].

In an attempt to create uniformity, the IEA-EBC Annex 67 [1] has, through an international collaboration, introduced flexibility functions, a novel methodology based on transfer functions to analyze an energy system's different sources of energy flexibility [15]. Such a flexibility function is the energy system's transfer function – i.e. change in energy use – to a change in a penalty function, such as the energy price. In contrast to flexibility indicators found in literature [14], these flexibility functions give a more comprehensive insight in the system's behaviour in case of a request for energy flexibility.

This work explores this proposed methodology by comparing two different TES systems (always) present in district heating networks, namely the thermal inertia of the buildings connected to the network

and the water thermal mass contained in the network pipes. To do so, optimal control problems are solved, each problem being different in the neighbourhood it considers and the TES system it uses to create energy flexibility. The solutions of these optimal control problems lead to step responses of the considered system in case of an energy flexibility call, which in turn results in the Annex 67's flexibility functions.

This paper first introduces flexibility functions and the corresponding step responses in more detail. Next, the methodology with which the corresponding step responses are determined and compared, is described. Finally, an overview of the results follows, along with a discussion of these results and main conclusions.

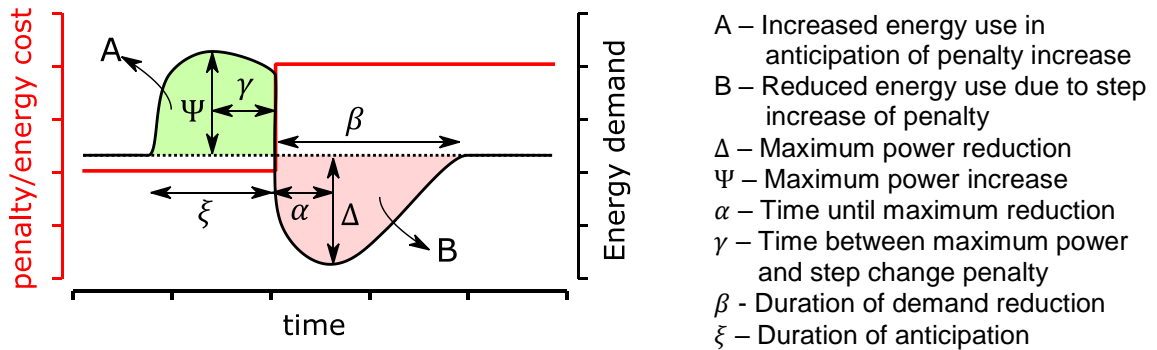


Figure 1: Graphical representation of the flexibility characteristics derived from the flexibility function as obtained using the direct results from an (anticipating) optimal control problem.

METHODOLOGY

This paper presents a direct calculation method of the flexibility function. This procedure does not rely on time series analysis to identify the flexibility function as described in [15], but directly computes the step response by solving two consecutive optimal control problems using a different cost/penalty signal:

1. A constant cost signal, which is considered the **reference** case.
2. A **step**-shaped cost signal, increasing the cost in the middle of the considered week from 1P/kWh to 2P/kWh (P is a fictitious unit to emphasize the artificial character of the penalty).

By subtracting the outcome of the first optimal control problem from that of the second, a similar profile is obtained to that of the step response in [15]. A theoretic representation of the profile, including the flexibility characteristics obtained from this profile, is shown in Figure 1. The main difference with the step response profile in [15] is caused by the optimization's anticipation of the penalty signal increase. Hence, the response already deviates from the reference signal before the penalty increase. As a result, determining the flexibility function through operational optimization can only be representative when (accurate) predictions of the penalty signal are available.

The optimization problems are compiled and solved with the help of the Python package *modesto* [16] and have a horizon of one week, as this period is sufficiently long to show all dynamics of a small thermal network (i.e. buildings and pipes). In case only the building dynamics are modelled (as will be explained further on), a discretization of 15 minutes is taken. If the pipe dynamics are modelled, a finer discretization of 5 minutes is taken to accurately model the propagation of water through the network pipes. The first week of the year is analysed in this paper, from the 1st to the 7th of January. This should be kept in mind when analysing the results, as these responses might be entirely different when considering another time period [14]. The weather conditions are taken from a data set [17] describing a representative year for the climate of Uccle, Belgium.

This paper focuses on the flexibility created by using a system's thermal inertia (originating from the building structure or the water contained in the network pipes). The next paragraphs outline the different scenarios that are implemented for respectively the neighbourhood and model cases.

Neighbourhood cases

Different district heating networks are analysed in this paper, three cases are on street level and two cases are on district level. The topologies are shown in Figure 2:

1. A **detached street** with 10 detached buildings,
2. A **mixed street** with 5 detached and 5 terraced buildings, giving a mix of buildings with a higher and lower UA-value,
3. A **terraced street** with 10 terraced buildings,

4. A **series district**, where 3 streets are all connected to the production unit through a single distribution pipe,
5. A **parallel district**, where 3 streets all have a separate pipe connecting them to the central production unit.

In the street cases, each of the 10 buildings is modelled separately, although buildings of the same type have identical models. The district cases consist of the combination of different streets, as is also shown in Figure 2. However, to reduce optimization problem complexity (which is justified for the study envisaged here), the aggregation scheme proposed by Patteeuw *et al.* [2] is applied. Using this scheme, each street is represented by a single characteristic building model. However, the used aggregation method neglects the street network pipes. Additionally, the aggregated building model of *Mixed Street* was approximated by choosing a building type that has a UA-value between that of the detached and the terraced building.

The building models are based on Belgian typologies as collected by Protopapadaki *et al.* [18]. The used types are listed in Table 1. The buildings' comfort requirements are based on the profiles described in the ISO13790 standard [19]. However, to create diversity amongst the different buildings and streets, some stochastic behaviour was added to the profile, changing the requested temperatures and absence/presence periods slightly. To provide energy flexibility an increase of the indoor temperatures by 1°C is allowed. Domestic hot water was left out of the models for now, but will be added in a future stage. The buildings in the network have a minimum required supply temperature of 60°C. The building substations are modelled as heat exchangers with a constant temperature difference across the primary side of 30°C. The pipes are sized according to the heat demand of the buildings and the recommendations made in the IsoPlus catalogue [20].

Table 1: A description of the building types used. For more information, see [18].

Building name	<i>Terraced</i>	<i>Detached</i>	<i>Mixed Street (Aggregated)</i>
Building type	Terraced Age: 2008-2012 UA-value: 217 W/K	Detached Age: 2008-2012 UA-value: 350 W/K	Semi-Detached Age: 2008-2012 UA-value: 285 W/K

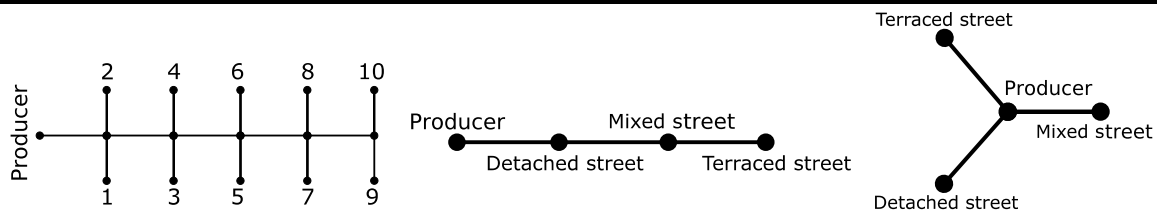


Figure 2: The topologies of the streets (left), series district (middle) and parallel district (right).

Model cases

Besides the neighbourhood composition, the cases also differ in the models that are applied to describe the district heating network in order to (un)lock different sources of flexibility. Table 2 presents the different model cases investigated in this paper.

For the buildings, two models are used:

1. A resistance-capacitance (**RC**) model, which is suited to model the thermal inertia of the building and hence gives access to the building thermal inertia's energy flexibility. These models are based on the work of Reynders *et al.* [21].
2. A **heat profile**, a deterministic profile that gives the heat extraction of a building from the network. This model is suited to prohibit the use of the energy flexibility of the building thermal inertia, and to ensure a linear program (LP) if the dynamic pipe model is used (see below).

There are three options to model the pipes:

1. An **ideal** pipe model, with no heat losses, no energy transport delays and no limits on mass flow rates through the pipes.
2. A **steady-state** pipe model [22] with heat losses and mass flow rate limits but assuming steady-state, i.e. the temperature in the pipes does not change through time. As the energy flexibility from the network pipes is based on changing the water temperature in the pipes, this model prohibits the use of the network's energy flexibility.
3. A **dynamic** pipe model [23] with heat losses and energy transport delays, offering the possibility to use the pipe's energy flexibility. However, if the pipe mass flow rates are unknown, use of

this model results in a mixed integer non-linear program (MINLP), which falls beyond the scope of this paper. If the mass flow rates are known, the resulting model is an LP.

As listed in Table 2 the *Buildings – ideal network* and *Buildings* cases consider the buildings' energy flexibility (both using the RC-model). *Buildings – ideal network* uses the ideal pipe model, and is hence equivalent to each building being perfectly connected to the central heat source, whereas the *Buildings* case takes into account the imperfectly insulated pipes and limited mass flow rates.

By taking the heat profile as the building model, the *Network* case no longer considers the building's available energy flexibility, and instead focuses on the network pipes' energy flexibility by using the dynamic pipe model. Case *Combined - LP* uses the same models as the *Network* case but uses different building heat profiles: the *Network* case uses heat profiles that correspond with the buildings reacting to the constant penalty signal, whereas the *Combined-LP* case uses heat profiles describing the buildings' response to the step penalty signal. Hence, *Combined - LP* first determines the buildings' response, followed by the pipes' response. A better alternative to *Combined - LP* would be to combine the building RC-model and the dynamic pipe model, as the optimization can then determine the two systems' energy flexibility at the same time. However, the combination of these two models results in an MINLP and solvers for such problems are far more complex and time-consuming. Hence, instead of the *Combined – MINLP* case, the *Combined - LP* is selected to give a first estimate of a possible cooperation between network pipes and buildings. However, further research will consider the MINLP case as well.

Table 2: An overview of the different model cases.

Name	Energy flexibility source	Building model	Pipe model
Buildings - ideal network	Buildings	RC-model	Ideal
Buildings	Buildings	RC-model	Steady-state
Network	Network pipes	Heat profile (no building flexibility)	Dynamic
Combined - LP	1) Buildings 2) network pipes	Heat profile (building flexibility)	Dynamic

RESULTS

Solving for all combinations of cases (2 penalty signals, 5 neighbourhoods and 4 model cases) leads to 40 optimizations. However, the final number of step responses to analyse is half this number as the step response is calculated by subtracting the reference penalty signal from the step penalty signal. An example of this calculation for both the *Buildings* and *Network* model cases is shown in Figure 3. **Error! Reference source not found..**

Figure 4 shows the remaining 20 step responses. The shape of these curves is similar to the example shown in Figure 1.

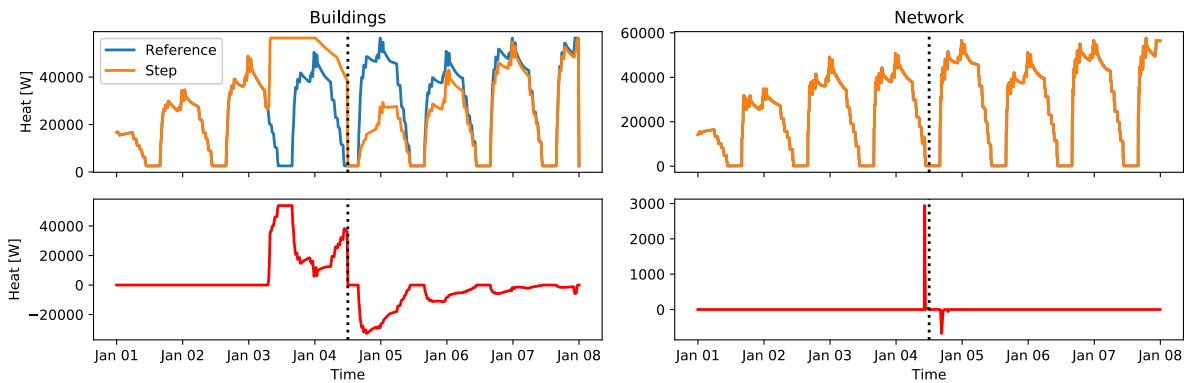


Figure 3: An example of a step response calculation for the *Buildings* and *Network* model cases for the *Terraced Street* case. The step response (lower plots) is calculated by subtracting the reference profile from the step penalty signal profile (upper plots). The vertical dotted lines indicate the position of the step increase in the penalty signal. Note that the left and right plots have different scales for the ordinates.

Buildings – network pipes comparison

A first notable result in Figure 4 is the difference between delivered flexibility when comparing the two *Buildings* cases to the *Network* case. The energy flexibility delivered by the network pipes is much smaller than that of the buildings, as is also confirmed in Table 3, which shows the total thermal inertia and UA-value of both network pipes and buildings separately and their combination. It can be concluded

that the pipes have a thermal inertia that is about a factor 1000 smaller. Their allowed temperature increase is higher, (10°C compared to 1°C for a building), though this is insufficient to counteract the smaller thermal inertia. This shows that the Annex 67 methodology produces results that are in line with expectations.

The pipes might deliver a more significant contribution to the total delivered energy flexibility, should they be able to co-operate with the buildings. One simplified case of such a co-operation is the *Combined - LP* case, which is a sequential co-operation between the buildings and the pipes. However, as Figure 4 shows, the difference between the *Combined - LP* case compared to the *Buildings* case remain small, even negligible. However, further conclusions regarding the possible cooperation between the network pipes and buildings can only be made after analysing the Combined MINLP case, which will be done in future research.

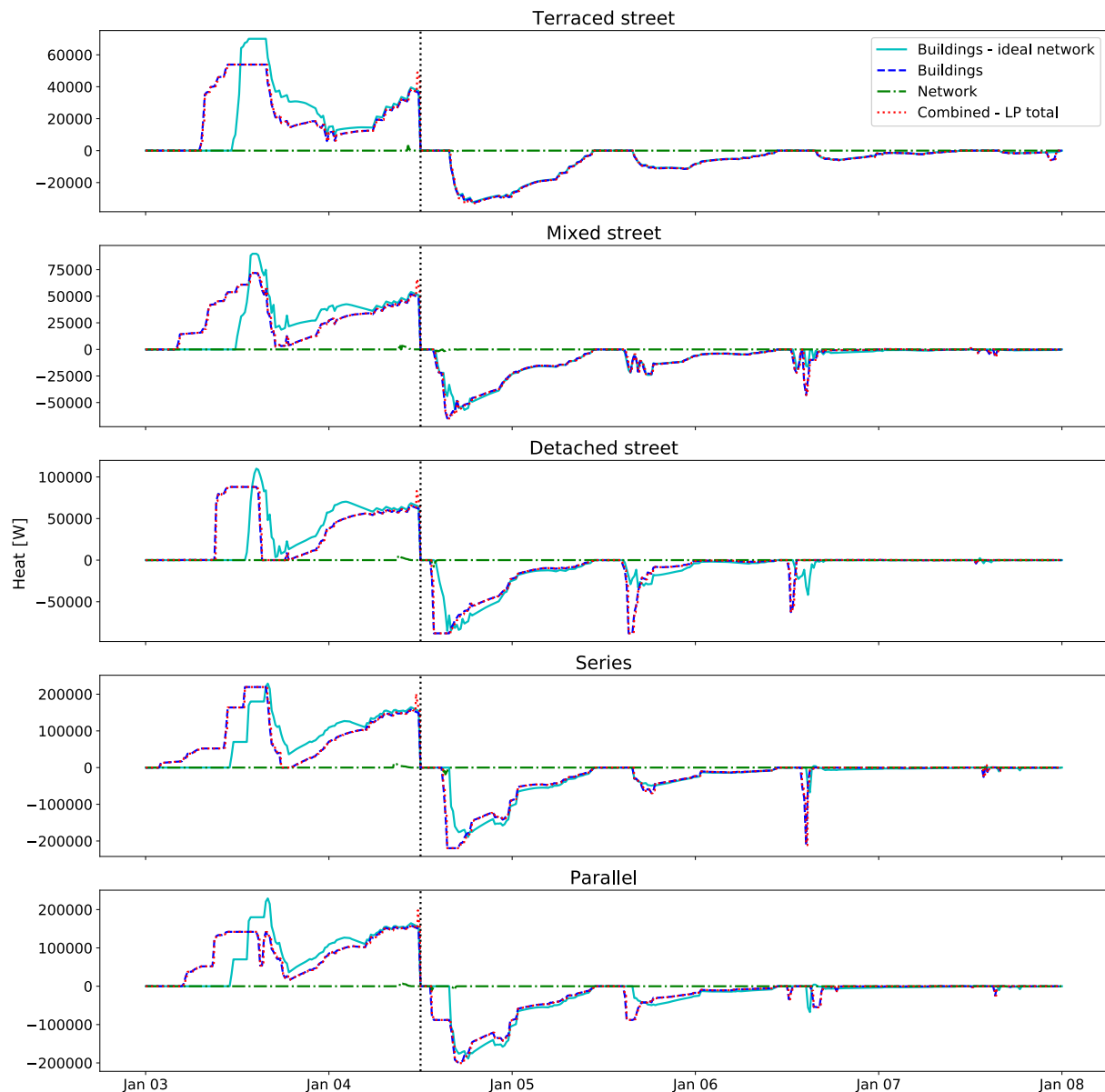


Figure 4: Step responses of each case. The first two days of the week are not shown as there is no response yet in any of the cases and it shows the interesting results more clearly.

Figure 4 also shows the minimum prediction horizon of the penalty signal (corresponding to the duration of anticipation ξ in Figure 1) that is needed to optimally use the available thermal inertia of the systems. The larger time constant of the buildings (see Table 4) causes this prediction horizon to be high when comparing it to the charging time of the network pipes. *Terraced street*, with large time constants (i.e. slow to cool down again), has the largest charging time. These buildings stay warm longer, and can start charging earlier, as most of the stored heat will still be present after the price increase. *Detached street* has buildings that have smaller time constants (i.e. quick to cool down again). These buildings

start charging later and hence have a smaller charging time, as these buildings are not as good in retaining the stored heat for a longer time period. These results confirm the findings of Reynders [11], leading to a further verification of the flexibility function method.

Table 3: The system capacitance and UA-value of the different district heating subsystems.

	Capacitance [kWh/K]			Total UA-value [W/K]		
	Network	Buildings	Combined	Network	Buildings	Combined
Terraced street	0.39	292	292	36.4	2170	2206
Mixed street	0.40	339	339	36.6	2835	2872
Detached street	0.42	386	386	36.8	3500	3539
Series district	1.28	944	945	43.7	8520	8564
Parallel district	0.54	944	944	38.4	8520	8558

Table 4: The time constants τ of the different district heating subsystems. Calculated with $\tau = RC$, R being the system thermal resistance and C the system thermal capacitance. [h]

	Network	Buildings
Terraced street	10.6	135
Mixed street	11.0	120
Detached street	11.3	110
Series district	29.3	111
Parallel district	14.0	111

Table 5: A comparison of the energy stored in the different subsystems (corresponding to A, see Figure 1) and the energy used (corresponding to B, see Figure 1) for all cases. Note that the difference between stored and used energy is caused by heat losses in the system. [kWh]

	Buildings - ideal network		Buildings		Network		Combined - LP	
	Stored	Used	Stored	Used	Stored	Used	Stored	Used
Terraced street	773.23	579.51	802.15	594.69	0.69	0.35	806.59	596.96
Mixed street	972.79	755.38	1022.87	785.07	2.92	1.68	1027.99	787.88
Detached street	1190.59	946.42	1227.38	971.87	3.92	2.62	1233.41	975.30
Series district	2883.15	2248.66	2913.23	2280.11	16.30	10.96	2929.63	2292.61
Parallel district	2883.15	2248.66	2900.12	2281.09	7.62	4.16	2907.94	2286.20

Comparison neighbourhood cases

Table 5 shows the energy that was stored in the system's available thermal inertia for the *Buildings* and *Network* cases. In the *Buildings* case, it can be seen that larger capacitances (see Table 3) cause a larger amount of stored energy. In the *Network* case, a clear (relative) difference can be seen as well. In the *Series district* case, this even leads to an increase of the used energy by a factor 2.6 when comparing it to the *Parallel district*, even though the difference in time constants (see Table 4) is only a factor 2.1. This difference is likely caused by the following aspects:

1. The sizing of the pipe: the larger sizes of the *Detached street* and the *Series district* cases (see Table 3), create a larger potential to store energy in the network, leading to higher amounts of stored energy.
2. The mass flow rates in the system: due to the *Series district* network topology and the resulting higher mass flow rates through each pipe compared to the *Parallel district*, water circulates faster through the *Series district*, making the energy spread out faster and giving more opportunity to charge the network.

Congestion

Another interesting aspect to study is whether flexibility functions of separate systems can be simply combined to form the response function of the overall system. If the system is linear, this should be the case, but one important aspect that makes thermal networks and energy systems in general non-linear, is congestion. In case of thermal networks, one example of congestion is the limitation on mass flow rates through the pipes to prevent excessive friction losses.

The consequences of congestion are shown in Figure 5. The inclusion of mass flow rate limits in the *Buildings* case causes a difference between the *Buildings – ideal network* and *Buildings* cases. In the latter case, the optimization has to limit the mass flow rates and consequently the heat injection into the network. This causes the charging of the network to start earlier in the *Buildings* case. This is shown in more detail for the *Mixed street* case in Figure 5. It is interesting to see the difference between the

charging of the terraced and detached buildings. In order to compensate for the congestion, the buildings are charged extra before the congestion period (the red zone in Figure 5). Afterwards, the detached buildings receive slightly more heat, most likely to counteract the faster cooling of these buildings. The terraced buildings on the other hand, receive less heat after the congestion period.

Hence, in case of a congested network, the step response of the street (*Buildings case*) is not the same as the sum of the step responses of the separate buildings (*Buildings – ideal network case*). This is in an important limitation of the flexibility function method as proposed by the IEA-EBC Annex 67, as one of the method's main advantages would be that the of sum of separate subsystems' flexibility functions lead to the combined system flexibility function . However, in case of congestion or another non-linearity, this relation is no longer valid.

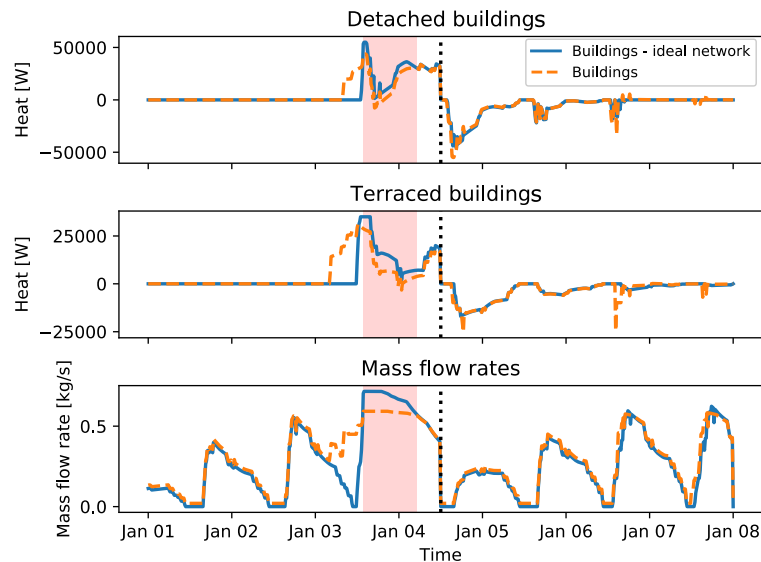


Figure 5: The decisions made in the Mixed street case. Both the Buildings - ideal network and the Buildings case are shown. The upper plot shows the heat extraction of all terraced buildings, the middle plot shows the heat extraction of all detached buildings. The lower plot shows the mass flow rates passing through the production unit. The congestion period is indicated by the red zones.

CONCLUSION

This work explored and verified flexibility functions (transfer functions, inspired by the work of IEA-EBC Annex 67) that can be used to quantify energy flexibility. The step responses corresponding to these transfer functions were used to analyse and compare the energy flexibility that can be delivered by the thermal inertia of both buildings and network pipes in district heating networks. To this end, different optimal control problems of several neighbourhoods, differing in type of buildings and network size, were solved. These optimal control problems also differed in the models they used to represent the district heating network, thereby (un)locking the energy flexibility of the thermal inertia of buildings and network pipes.

Analysis of these different cases showed that the flexibility that can be delivered by the network pipes is limited, certainly compared to the flexibility delivered by the buildings' thermal inertia. These and other results that can be derived from the flexibility functions are in accordance with results obtained in previous research, leading to a verification of the proposed flexibility function methodology. However, an important limitation of the methodology became apparent. In case of congestion, the behaviour of the subsystems changes in order to deal with the congestion caused by e.g. mass flow rate limits. This change in behaviour causes the separate step responses to no longer sum up to the overall system response, limiting the applicability of the methodology.

ACKNOWLEDGMENT

The authors would like to acknowledge the work done in the IEA–EBC Annex 67 project. This study is part of the research project “Towards a sustainable energy supply in cities”. This project receives the support of the European Union, the European Regional Development Fund ERDF, Flanders Innovation & Entrepreneurship and the Province of Limburg. The authors also would like to acknowledge the financial support of VITO for the PhD Fellowships of Bram van der Heijde and Annelies Vandermeulen.

REFERENCES

- [1] S. Ø. Jensen *et al.*, “IEA EBC Annex 67 Energy Flexible Buildings,” *Energy Build.*, vol. 155, pp. 25–34, 2017.
- [2] D. Patteeuw and L. Helsen, “Residential buildings with heat pumps, a verified bottom-up model for demand side management studies,” *9th Int. Conf. Syst. Simul. Build.*, no. 1, pp. 1–19, 2014.
- [3] E. Guelpa, G. Barbero, A. Sciacovelli, and V. Verda, “Peak-shaving in district heating systems through optimal management of the thermal request of buildings,” *Energy*, vol. 137, pp. 706–714, 2017.
- [4] D. Vanhoudt, D. Geysen, B. Claessens, F. Leemans, L. Jespers, and J. Van Bael, “An actively controlled residential heat pump: Potential on peak shaving and maximization of self-consumption of renewable energy,” *Renew. Energy*, vol. 63, pp. 531–543, 2014.
- [5] D. Basciotti, F. Judex, O. Pol, and R. Schmidt, “Sensible heat storage in district heating networks : a novel control strategy using the network as storage,” in *Conference proceedings of the 6th international renewable energy storage conference IRES*, Berlin, Germany, 2011.
- [6] E. Carpaneto, P. Lazzeroni, and M. Repetto, “Optimal integration of solar energy in a district heating network,” *Renew. Energy*, vol. 75, pp. 714–721, 2015.
- [7] T. Korpela *et al.*, “Utilization of District Heating Networks to Provide Flexibility in CHP Production,” *Energy Procedia*, vol. 116, pp. 310–319, 2017.
- [8] J. Salpakari, J. Mikkola, and P. D. Lund, “Improved flexibility with large-scale variable renewable power in cities through optimal demand side management and power-to-heat conversion,” *Energy Convers. Manag.*, vol. 126, pp. 649–661, 2016.
- [9] J. Kensby, A. Trüschel, and J.-O. Dalenbäck, “Potential of residential buildings as thermal energy storage in district heating systems – Results from a pilot test,” *Appl. Energy*, vol. 137, pp. 773–781, 2015.
- [10] S. Stinner, K. Huchtemann, and D. Müller, “Quantifying the operational flexibility of building energy systems with thermal energy storages,” *Appl. Energy*, vol. 181, pp. 140–154, Nov. 2016.
- [11] G. Reynders, “Quantifying the impact of building design on the potential of structural storage for active demand response in residential buildings,” PhD thesis, KU Leuven, 2015.
- [12] R. De Coninck and L. Helsen, “Quantification of flexibility in buildings by cost curves – Methodology and application,” *Appl. Energy*, vol. 162, pp. 653–665, Jan. 2016.
- [13] B. van der Heijde, M. Sourbron, F. J. Vega Arance, R. Salenbien, and L. Helsen, “Unlocking flexibility by exploiting the thermal capacity of concrete core activation,” in *11th international Renewable Energy Storage Conference*, Düsseldorf, Germany, 2017.
- [14] G. Reynders, R. Amaral Lopes, A. Marszal-Pomianowska, D. Aelenei, J. Martins, and D. Saelens, “Energy flexible buildings: An evaluation of definitions and quantification methodologies applied to thermal storage,” *Energy Build.*, vol. 166, pp. 372–390, 2018.
- [15] R. Grønborg Junker *et al.*, “Characterizing the energy flexibility of building and districts,” *Submitt. to Appl. Energy*, 2018.
- [16] A. Vandermeulen, B. van der Heijde, D. Patteeuw, D. Vanhoudt, R. Salenbien, and L. Helsen, “modesto - a Multi-Objective District Energy Systems Toolbox for Optimization,” in *5th International Solar District Heating Conference*, Graz, Austria, 2018.
- [17] S. Wilcox and W. Marion., “User’s Manual for TMY3 Data Sets, NREL/TP-581-43156.”, 2008.
- [18] C. Protopapadaki, G. Reynders, and D. Saelens, “Bottom-up modelling of the Belgian residential building stock: impact of building stock descriptions,” in *9th International Conference on System Simulation in Buildings*, Liege, Belgium, 2014, vol. 2, no. 1, pp. 1–21.
- [19] International Organization for Standardization., *ISO 13790:2008 Energy performance of buildings -- Calculation of energy use for space heating and cooling*. Geneva, Switzerland, 2003.
- [20] Isoplus, “Isoplus product catalog.” 2016.
- [21] G. Reynders, J. Diriken, and D. Saelens, “Bottom-up modeling of the Belgian residential building stock : influence of model complexity,” in *9th International Conference on System Simulation in Buildings*, Liege, Belgium, 2014, vol. 2, no. 1, pp. 1–19.
- [22] B. van der Heijde, A. Aertgeerts, and L. Helsen, “Modelling steady-state thermal behaviour of double thermal network pipes,” *Int. J. Therm. Sci.*, vol. 117, pp. 316–327, Jul. 2017.
- [23] A. Bennonysson, “Dynamic Modelling and Operation Optimization of District Heating Systems,” PhD thesis, Technical University of Denmark (DTU), 1991.